Design, Simulation and Kinematic Verification of A Multi-Loop Ankle-foot Prosthetic Mechanism

Majun Song, *Member, IEEE*, Zhongyi Li, Weihai Chen, Hao Zheng, Sheng Guo, John Rasmussen, and Shaoping Bai, *Senior Member, IEEE*

***Abstract*—Inspired by the bionic characteristics of ankle and calf skeletal muscles, a novel ankle-foot prosthesis (AFP) with variable stiffness mechanisms (VSMs) is proposed to assist transtibial amputees to restore ankle plantarflexion-dorsiflexion. The prosthesis is designed in the form of a spring-loaded three-loop linkage for function of continuous energy absorption-release in gait stance phase, which can facilitate ankle plantarflexion-dorsiflexion and keep human body move forward steadily. A compliant crank slider mechanism is also developed to power-assist AFP mechanism to improve the adaptive compliant contact between prosthesis and ground. In this paper, mechanics models of the ATP are developed to reveal the variable moment of the ankle joint, which is verified by human-machine simulation. An AFP prototype is built to validate the design experimentally. The results demonstrate that the AFP mechanism has the advantages of low power consumption, human-like joint moment profile. In particular, it is shown that the AFP mechanism with 54W power provided in toe-off phase can reduce the peak power of the motor by 24%.**

***Index Terms*—Ankle-foot prosthetic mechanism, Human biomechanics, Three-loop linkage mechanism, Compliant crank slider mechanism, Mechanical Self-adaptivity, Variable stiffness mechanism**

I. Introduction

WARS, diseases, natural disasters and accidents are the major causes of lower limb amputations, especially the number of transtibial amputees [1-3]. Ankles play important roles for support in the stance phase of gait and to move the body forward at the end of the stance phase; injury or loss of ankles affect ambulation ability, activities of daily living and quality-of-life. Design and optimization of prostheses for transtibial amputees is therefore an important task [4-5].

Passive robotic prostheses have been optimized for weight and cost, but extra metabolic energy is needed for the amputees to lift prosthesis off from the ground [6-7], which will cause discomfort, fatigue, and exclusion to the amputees' activities. Powered ankle prostheses have been investigated to address these shortcomings. Grimmer [8] designed a powered ankle prosthesis, which has motion modes of standing, walking and running, and its reduction of metabolic energy consumption in stance phase is verified experimentally. However, the motors and reducers add size and mass to the prostheses, which will affect gait coordination and stability, and increase energy consumption in swing phase. To solve these problems, Herr [9-10], Jimenez [11-12] and Geeroms [13] adopted spring devices in ankle prostheses to provide power in toe-off phase. This approach can decrease peak power of the motors and also reduce their size and weight, that's to say, the serial and parallel elastic devices have been used in the prosthetics to provide energy in recent years. However, these springs or elastic devices developed by open single-loop structures can only have energy supply at end of stance phase and cannot mimic agonist-antagonist function of articular skeletal muscles effectively [14]. Moreover, their stiffness characteristic does not match the human ankle stiffness during walking, which limits the dynamic performance of AFP mechanism as a prosthesis. It is noted that there are some VSMs designed with single-loop mechanism and springs [15-16], which can achieve variable stiffness in adjustable ranges by tracking the human-like joints' motion and have been used in exoskeletons.

In this paper, a novel AFP is developed incorporating a new VSM of a three-loop mechanism to overcome the aforementioned issues. The three-loop mechanism with two anisotropic springs (TLMS device) can synchronously mimic working function of the tibialis anterior and triceps surae muscles in dorsiflexion and plantarflexion respectively. This VSM features the compact and lightweight structure which facilitates the periodic motion of AFP mechanism by releasing energy, while residual energy is recycled and used in the subsequent gait phase. Moreover, the layout of two springs can prevent excessive forwarding tilt of the center of gravity in the early stance phase, and promote dorsiflexion of the AFP mechanism to clear the ground in swing phase. To provide sufficient energy for AFP mechanism and reduce the peak power of its motor in final toe-off phase, a spring-loaded, parallel, compliant crank slider mechanism (CCSMP device), which adopts a flexible hinge for prosthetic toe, is proposed.

The paper is organized as follows: Sec. II presents the design

This work was supported in part by the Key Research and Development Program of Zhejiang Province under Grant No. 2021C03050, in part by the National Natural Science Foundation of China under Grant No. 52305004, in part by the China Postdoctoral Science Foundation under Grant No. 2023M740193, in part by the Zhejiang Provincial Natural Science Foundation of China under Grant No. LQ24E050008, in part by the National Natural Science Foundation of China under Grant No. 51875033.

(Corresponding author: Weihai Chen, Sheng Guo)

Majun Song, Zhongyi Li, Hao Zheng, and Weihai Chen are with Hangzhou Innovation Institute, Beihang University, Hangzhou 310051, P. R. China (e-mail: mjsong1105@126.com; 1225234532@qq.com; haozheng@zju.edu.cn; whchenbuaa@126.com)

Sheng Guo is with the Robotics Research Center, School of Mechanical, Electronic and Control Engineering, Beijing Jiaotong University, Beijing 100044, P. R. China (e-mail: shguo@bjtu.edu.cn).

John Rasmussen and Shaoping Bai are with the Department of Materials and Production, Aalborg University, Aalborg 9220, Denmark (e-mail: jr@mp.aau.dk; shb@mp.aau.dk).

principles based on human kinesiology; an AFP mechanism is designed. Sec. III describes modeling of the AFP. Simulation results are presented in Sec. IV. In Sec. V, a prototype is described, with which its kinematic performance is experimentally studied. The work is concluded and discussed in Sec. VI.

II. Conceptual Model of AFP Mechanism

A. Design Requirements

The dominant motion of ankle in gait cycle is plantarflexion and dorsiflexion, which is the focus of prosthetic mechanism in this paper. As shown in literatures [17-19], the ankle plantarflexion-dorsiflexion is mainly realized by contraction of the triceps surae (No. 1 and No. 3 in Fig. 1) and tibialis anterior (No. 2 in Fig. 1) muscles [20-21].

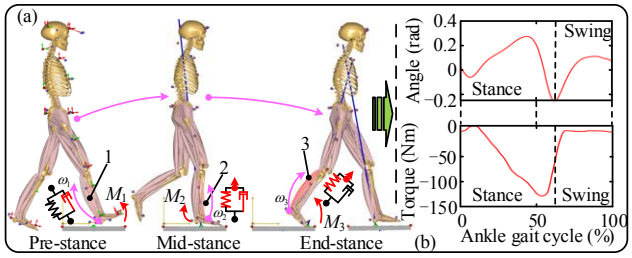

Fig.1. Biomechanical mechanism of human walking. (a) Kinesiology and biomechanics, (b) ankle motion and moment.

In this work, a bio-inspired AFP mechanism is proposed to assist the transtibial amputees recovering their lost ankle physiologic characteristics (Fig.1a), as follows.

1) Physiological modulation of ankle kinematics and dynamics during level-ground walking, i.e. coupled relationship between joint angular position and its moment acted by skeletal muscles.

2) Biomechanical compatibility and evaluation of human-like joint impedance and dynamics, i.e. compensation mechanism between energy devices and human skeletal muscles.

To achieve these goals, the following design requirements of bionic devices are determined:

1) An energy device based on multi-link mechanism is proposed, which can generate dorsiflexor moment to promote a steady forward movement of the human body in foot-flat, and form plantarflexor moments to prevent human from leaning forward too much after heel-off phases. That's to say, multi-link mechanism integrated functions of energy storage and damping, which is inspired by muscles agonist-antagonist.

2) Inspired by the power-assisted characteristics of flexible toe joint and extensor digitorum/ hallucis longus, another energy device with flexible hinge is implemented to assist prosthetic foot lifting from ground in toe-off II phase with extra ankle plantarflexor moment and toe extensor moment, as well to adapt different terrains and enhance cushioning comfortability.

Besides, a damping device should be used at the heel to mitigate the impact of AFP mechanism in heel strike, meanwhile, a dorsiflexor moment will be generated.

B. Proposed Prosthetic Mechanism

The schematic diagram of TLMS and CCSMP devices in AFP mechanism are shown in Fig. 2. The TLMS and CCSMP devices work independently during walking gait cycle, the working state of former depends on the position of ankle joint, and the latter depends on the position of ankle and toe joints.

Fig. 3 displays the CAD model of AFP mechanism. The AFP mechanism, which has motion function of ankle dorsiflexion-plantarflexion, is mainly composed of motor module, mounting base, spring cushion system, TLMS device, CCSMP device, circular adaptive block (CAB device), carbon fiber prosthetic foot and sensors for the measurement of ankle angle and foot pressure.

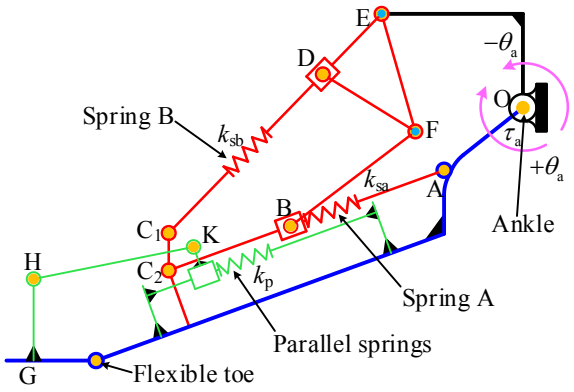

Fig.2 Schematic of AFP mechanism with two VSMs. Solid black line denotes the fixed base, blue dotted line is the prosthetic foot including prosthetic toe which is connected by flexible toe, solid red line is the TLMS device, and dashed green line is the CCSMP device.

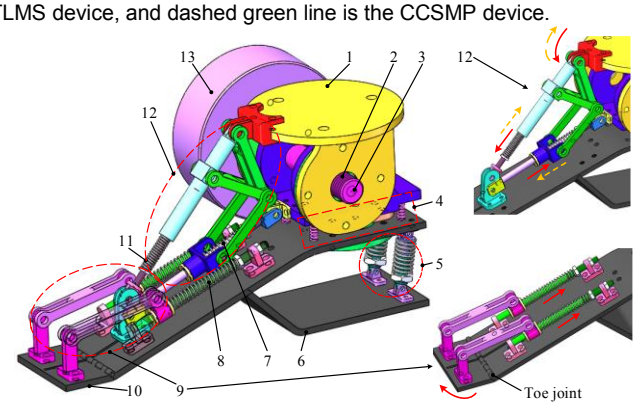

Fig.3. A conceptual model of AFP mechanism, (1) Base, (2) Actuating axis, (3) Angle sensor, (4) CAB device, (5) Spring cushion system, (6) Carbon fiber prosthetic foot, (7) Spring A, (8) Parallel springs, (9) CCSMP device, (10) Pressure sensor, (11) Spring B, (12) TLMS device, (13) Motor.

In the AFP mechanism, spring cushion system can primarily cushion and absorb shock in heel-strike phase, and also assist the AFP mechanism to transfer from heel-strike to flat-foot phase. The TLMS device works in the gait cycle and two springs imitate the anterior tibial muscle and gastrocnemius when the AFP mechanism in dorsiflexion and plantarflexion respectively, i.e., Spring A contracts like gastrocnemius when the AFP mechanism in plantarflexion while Spring B relaxes, and Spring B contracts like anterior tibial muscle when the AFP mechanism in dorsiflexion. TLMS device has functions of continuous energy absorption-release inspired by the agonist-antagonist articular skeletal muscles. The parallel springs of CCSMP device begin to be contracted when the toe rotates in heel-off phase. They will be released in toe-off II phase when the AFP lifts from the ground.

C. Multi-loop Structural Design

Two unidirectional compression springs, namely, Springs A and B that are adopted in TLMS device are shown in Fig. 4.

During the dorsiflexion-plantarflexion of AFP mechanism, one compression spring releases the stored energy to assist the AFP mechanism to switch rotational mode easily, and the other one begins to store the energy simultaneously.

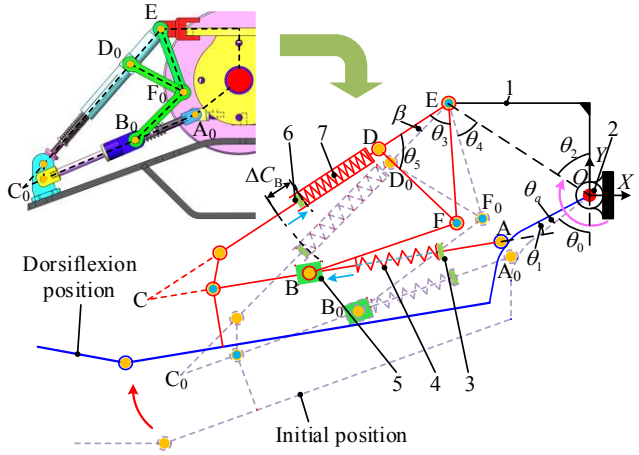

Fig.4. Structural diagram of TLMS device. (1) Fixed base, (2) Motor, (3) Nut 1, (4) Spring A, (5) Slider 1, (6) Nut 2, (7) Spring B.

In Fig. 4, the AFP mechanism is mainly in dorsiflexion at the end of flat-foot phase, as well as in heel-off phase. The motor rotates clockwise to drive the TLMS. At the beginning of flat-foot phase, the partial energy released to help the AFP mechanism complete the rotation mode switch from plantarflexion to dorsiflexion. Meanwhile, the slider 1 moves away from Spring A, with increasing dorsiflexion angle in heel-off phase, Spring B is compressed by nut 2 and the elastic energy is stored. Besides, Spring B can also prevent the human body from leaning forward excessively.

The stored energy is released from the end of heel-off phase, which assists the AFP mechanism to switch its rotation modes at the beginning of toe-off I phase. At this moment, Spring A is compressed by slider 1, which begins to store the elastic energy. The AFP mechanism is mainly in plantarflexion in the middle of toe-off-II phase, while the motor drives the TLMS device to rotate counterclockwise. With the plantarflexion angle increasing, the stored energy is released by Spring A for the AFP mechanism to lift the prosthesis from the ground at the end of toe-off-II phase. Besides, Spring A is fitted with nut 1 to adjust spring pretension according to the required energy.

III. Design Modeling and Analysis

The two devices with multi-loop mechanism presented in Sec. II are modeled to reveal their kinematic and stiffness characteristics that are compatible with human beings.

A. TLMS Device

Referring to Fig. 4, the positions of A and E are known, we can then get new position of point A and point C after rotating θ_a, as well as the length of l_{EC0}, l_{EC} and l_{CC0}.

$$\begin{cases} x_A = -l_{OA}\sin(\theta_0+\theta_a) \\ y_A = -l_{OA}\cos(\theta_0+\theta_a) \end{cases}, \begin{cases} x_C = x_A - l_{AC}\sin(\theta_0+\theta_1+\theta_a) \\ y_C = y_A - l_{AC}\cos(\theta_0+\theta_1+\theta_a) \end{cases} \quad (1)$$

where θ_a is ankle rotation angle. It is positive when ankle dorsiflexion and negative when ankle plantarflexion.

According to the equilibrium of forces between the elastic force F_B generated by Spring B and joint moment of AFP mechanism, the joint stiffness k_B can be derived as

$$k_B = \frac{T_e(\theta_a,\beta)}{\Delta C_B \cdot l_{OE}\sin(\pi-\theta_3-\theta_4-\beta)} \quad (2)$$

where ΔC_B is the compression of Spring B. T_e is required moment when ankle is in maximum dorsiflexion from initial position. Rotational angle β of CE around point E can be represented in plantarflexion:

$$\beta = \arccos\frac{l_{CE}^2 + l_{C_0E}^2 - l_{C_0C}^2}{2 l_{CE} l_{C_0E}} \quad (3)$$

According to the equilibrium of forces between the elastic force F_A generated by spring A and joint moment of AFP mechanism, the joint stiffness k_B is

$$k_A = \frac{T_f(\theta_a,\beta,p_A)}{\Delta C_A \cdot l_{OA}\sin(\theta_1)} \quad (4)$$

where ΔC_A is the compression of spring A. p_A denotes the pretension of spring A. T_f is one of the required moment when the ankle been in maximum plantarflexion.

From Eqs. (2) and (4), we can find that TLMS device has variable stiffness characteristics with respect to the motion of ankle plantarflexion-dorsiflexion, which is required for the design of elastic devices in prosthetic mechanism.

B. CCSMP Device

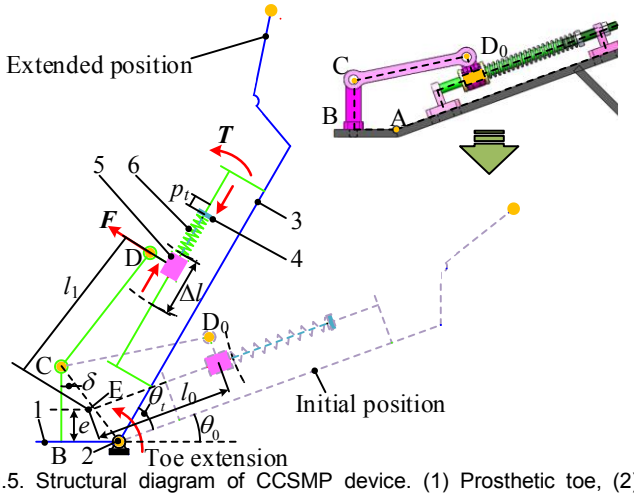

Fig.5. Structural diagram of CCSMP device. (1) Prosthetic toe, (2) Flexible hinge, (3) Prosthetic foot, (4) Nut 3, (5) Slider 2, (6) Parallel springs.

The CCSMP device aims to provide more power in toe-off II phase. A compliant hinge [22-23] is adopted as the toe joint in the CCSMP device, as shown in Fig. 5, the compliant toe and the parallel springs can be acted as an agonist-antagonist structure to mimic the biomimetic muscles' function by the movements of toe joint. Different from the existing powered prosthetic toe with complex control system [24], the CCSMP device has the advantages of simple structure, human-like flexibility and autonomous self-adaptive capacity.

1). Variable stiffness of Parallel Springs

During support phase including heel-off and toe-off phases, the rotation angles of the hip, knee and ankle in sagittal plane are θ_h, θ_k and θ_a respectively, the relationship between rotation angle of the toe and each angle of the lower limb is expressed.

$$\theta_t = \theta_h + \theta_k + \theta_a + \eta \quad (5)$$

where η denotes the safe angle of excessive rotation of the toe in toe-off phase. In order to adapt the prosthetic foot to the movement of different lower limbs, it takes $\eta \approx 8°$.

The position of point D moves upward when the toe begins to rotate from HO phase to TO-II phase. Its new position will be calculated for any toe angle θ_t. The length between point D and prosthetic toe can be derived as,

$$l_1(\theta_t) = l_{CE}\sin(\xi) + l_{CD}\sqrt{1-\left(l_{CE}l_{CD}^{-1}\cos(\xi)\right)^2} \tag{6}$$

where ξ is equal to the sum of δ, θ_t and θ_0.

The stiffness coefficient of parallel springs, k_t, can be calculated by Eq. (7). Likewise, the parallel springs also have the variable stiffness characteristics with respect to the movements of hip, knee, ankle and toe joints.

$$k_t = \frac{F_t(\theta_t, p_t)\cdot l_{CD}\sqrt{1-\left(l_{CE}l_{CD}^{-1}\cos(\xi)\right)^2}}{l_{CE}\cos(\xi)\cdot\Delta l} \tag{7}$$

where $F_t(\theta_t, p_t)$ denotes the pressure generated by the spring force, and the direction is perpendicular to DE and up. Δl denotes the compressed displacement of the spring. p_t denotes the displacement of the spring under the preload force.

The parallel springs in CCSMP device only work from HO to TO-II phases, i.e., the parallel springs are compressed after foot rotating around the toe joint, and the kinetic energy of foot is converted into elastic energy to lift the foot from the ground. Furthermore, CCSMP device is suitable for different amputees by adjustment of the spring preload force.

2). Stiffness Requirement of Compliant Toe Joint

Fig. 6 shows the schematic diagram of prosthetic foot with a flexible toe joint, which is built by 1R pseudo-rigid body. O is the position of foot's center of mass which is the origin of global coordinate system, A is toe's position, and B is toe's center of mass. ψ is pseudo rigid body angle which can be approximated as toe's extension angle. Considering the similarity between large deformation of the flexible toe end and the trajectory of toe tip round toe joint, characteristic radius coefficient λ is introduced [23] and the geometric size of toe AB can be determined as λd. Thus, the dimensionless coordinates of B can be expressed in global coordinate system, and the pseudo-rigid body angle also can be derived as

$$\begin{cases} B_x = \dfrac{x}{d} = 1-\lambda(1-\cos\psi) \\ B_y = \dfrac{y}{d} = \lambda\sin\psi \end{cases}, \quad \psi = \arctan\frac{b}{a+d(\lambda-1)} \tag{8}$$

The flexible hinge in the 1R pseudo-rigid body causes the angle of the pseudo-rigid body approximately equal to the rotational angle of B, i.e. $\psi \approx \theta$. To ensure the accuracy of the rotational trajectory, the rotational angle of the toe should be limited within an allowable extreme angle, which is expressed as ψ_{max}. An optimized numerical model of λ and ψ can be built.

$$\begin{cases} Find: \lambda \\ Min: \dfrac{1}{\psi} \\ S.T.: f(\psi) = \dfrac{|\theta_e|}{\theta} \le \left|\dfrac{\theta_e}{\theta}\right|_{max} = \delta_{max} \\ \lambda \in (0,\ 1) \end{cases} \tag{9}$$

where $\theta_e = \psi - \theta$ is the absolute angular error. ψ is the rotational angle of the center of gravity of toe. Δ_{max} denotes the maximum permissible error. We set δ_{max}=1% in this model.

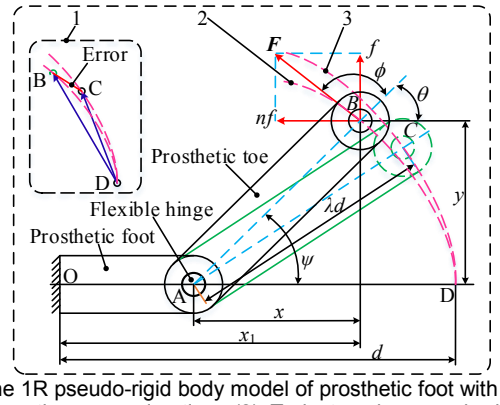

Fig. 6 The 1R pseudo-rigid body model of prosthetic foot with toe joint. (1) Deformation approximation, (2) Trajectory by pseudo-rigid body model, (3). Trajectory by elliptic integration.

In toe-off phase, the direction of ground reaction force exerted on the toe points to the center of gravity of human body and the angle is 10° with the vertical direction. To ensure the safety and reliability, the direction of the ground reaction force exerted on the toe is defined as vertically upward. Therefore, the ground reaction force exerted on the center of mass of the toe is perpendicular to the toe and φ is 90°. The search step to the rotational angle is set as $\Delta\theta$=0.01 and the optimal solution is found as $\lambda \approx 0.815$ by three-dimensional search [24, 25]. Meanwhile, the allowable extreme angle is found as $\psi_{max} \approx 72.2°$, which is greater than θ_t. The feasibility of optimal solution of characteristic radius coefficient is thus verified.

The stiffness of the flexible hinge in the pseudo-rigid model can be determined as follow:

$$k_{toe} = \lambda k_\psi \frac{EI}{d} \tag{10}$$

where k_{toe} denotes the structural stiffness. E is the Young's modulus of the carbon fiber. I is the inertia constant of pseudo-rigid model. k_ψ is a stiffness coefficient based on the angle generated by pseudo-rigid body, which is a constant taken as $k_\psi \approx \lambda\pi$. Finally, the torsional stiffness of the flexible hinge can be determined, which is $k_{toe} \approx 14.60$Nmm/deg.

IV. Simulation

The TLMS and CCSMP devices are crucial parts in AFP mechanism which can mimic the working performance of ankle's skeletal muscles in gait cycle and provide energy for the AFP mechanism. As can be seen in Sec. III, the TLMS device has variable stiffness characteristics with respect to the movement of ankle, and the CCSMP device also has the variable stiffness characteristics with respect to the movement of hip, knee, ankle and toe joints.

The structural parameters of TLMS and CCSMP devices in AFP mechanism are determined, as listed in Tab.I. The free end of Spring A in TLMS device is set preload force with the compressed distance of p_A= 5mm. The CCSMP device works from HO phase to TO-II phase and the rotation angles of hip, knee and ankle in the sagittal plane are θ_h=−18.01°, θ_k=−28.64°, θ_a=9.32° based on the experimental testing.

TABLE I
STRUCTURAL PARAMETERS OF TLMS AND CCSMP DEVICES

Devices	Parameters	
	Length (mm)	Angle (deg)
TLMS	l_{OA}=37, l_{OE}=62.5, l_{AC}=$l_{A_0C_0}$=110, l_{DE}=l_{D_0E}=31, l_{EF}=$l_{E_0F_0}$=l_{FB}=$l_{F_0B_0}$=45, l_{DF}=40, l_{C_0E}=120.	θ_0=51.5, θ_1=18.5, θ_2=56.5, θ_3=60, θ_4=37.
CCSMP	l_{AB}=22.5, l_{BC}=28, l_{CD}=l_{CD_0}=60, E=14.	θ_0=18, δ=39.

TABLE II
MECHANICAL PROPERTIES OF SPRINGS IN CCSMP DEVICE

Springs	Spring A	Spring B	Parallel Springs
compression	Δx_A≈9.90 mm	Δx_B≈13.69 mm	Δx_P≈39.29 mm
forces	F_A≈1425.17 N	F_B≈2052.52 N	F_P≈2555.51 N
stiffness	170 N/mm	150 N/mm	65 N/mm
work phase	HO	TO-II	TO-II
motion	plantarflexion	dorsiflexion	plantarflexion
value	θ_a≈ −9°	θ_a≈ 15°	θ_t≈ 45°

In this work, the human-machine model consists of a human musculoskeletal model with transtibial amputee and an AFP mechanism, and its inverse dynamic simulation is performed during the human-like walking of this model, as shown in Fig.7.

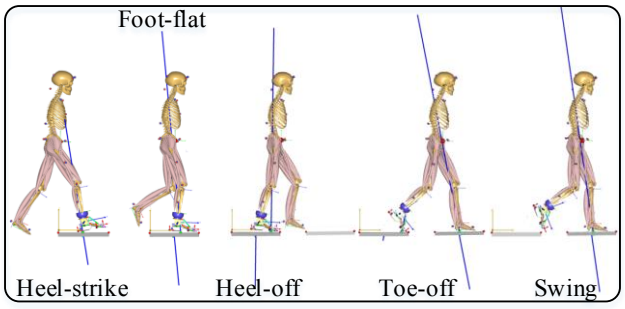

Fig. 7. Walking dynamics analysis of human- prosthetic mechanism in a gait cycle.

Fig. 7 presents the walking process of human-machine system in a gait cycle. The system can experience heel-strike, foot-flat, heel-off, toe-off and swing phases during human-like walking successfully without kinematic and dynamical calculation error. The solid blue line represents the ground reaction force when the model walking on the ground, and the length of the solid blue line indicates the amplitude of the ground reaction force exerted on the foot.

The parameters of the springs used in TLMS and CCSMP devices are listed in Tab. II.

A. Mechanical Performance

The comparison of ankle biomechanical performance in gait stance phase between healthy human, theoretical result and AFP mechanism is shown in Fig. 8. The green dashed line presents the relationship between the ankle moment and ankle angular position measured from the able-bodied subjects [26] in walking gait cycle, which is the desired reference of biomechanical performance for the development of ankle prosthetic mechanism. The red solid line denotes the ankle moment and ankle angular position of AFP mechanism obtained by simulation on human-machine walking interaction platform of AnyBody Modeling System, besides, its theoretical calculation has also been provided according to the derivation of ankle stiffness in Section III which is represented by blue dotted line.

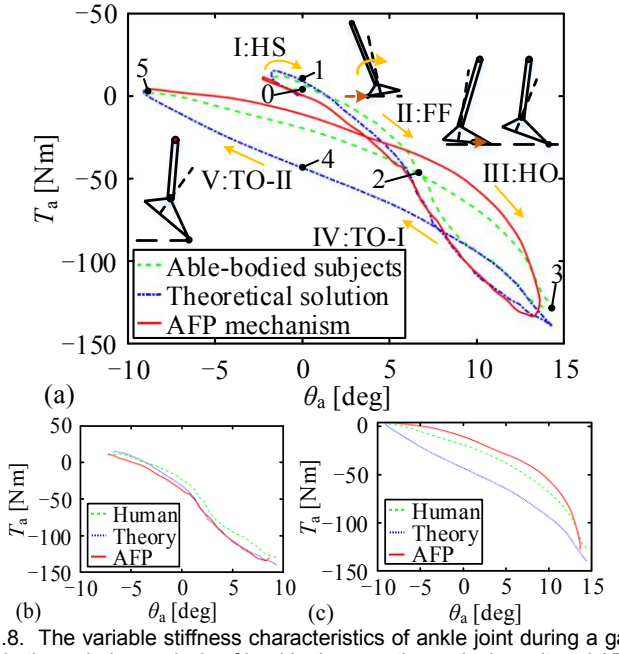

Fig.8. The variable stiffness characteristics of ankle joint during a gait cycle through the analysis of healthy human, theoretical result and AFP mechanism. (a) Ankle moments of AFP mechanism under the working VSMs, (b) ankle moments versus angles under Spring B in TLMS and CCSMP device during foot flat and heel off phases, (c) ankle moments in toe off phase.

An obvious difference is noticed in the variation trend of moment-angle relationship between the theoretical result and able-bodied subjects, especially in the toe off phase, as shown in Fig. 8(c). This is because geometric errors are existed in the theoretical modeling which is compared with the human structure, and the theoretical model is also an idealized model that ignores the biomechanical functions of muscles. Due to the energy-damping performance of the TLMS device and moment-assisted function of CCSMP device, AFP mechanism behaves similarly with the able-bodied subjects. The results also show that the biomechanical characteristics of AFP mechanism matches with that of able-bodied subjects. Meanwhile, Figs. 8(b) and 8(c) illustrate torque-deflection relationship of the VSMs used in the AFP mechanism, the results show that the AFP mechanism has the variable stiffness characteristic in different gait phase.

Moreover, Fig. 8 shows the AFP mechanism produces positive (dorsiflexor) moment in the heel-strike phase and negative (plantarflexor) moment between the flat foot phase and heel off phase. The results explain that the spring cushion system, TLMS and CCSMP devices work with the ankle movement in gait stance phase and thus meet the design requirements.

B. Power and Metabolic Consumption

The compression spring A and the parallel springs in CCSMP device release the stored elastic potential energy at the end of toe-off-II phase, which translates into sufficient useful power for the AFP mechanism to lift from the ground. The power contribution of the driving motor, TLMS device and CCSMP device in AFP mechanism are shown in Fig.9.

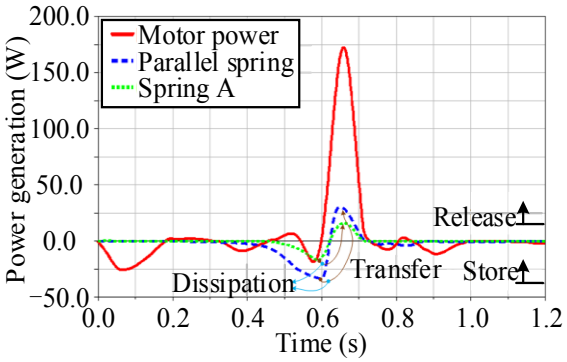

Fig. 9. Power distribution in AFP mechanism

Due to the adoption of TLMS and CCSMP devices, the required peak power of motor decreases from 244.20W to 172.86W, while each compression spring in CCSMP device and Spring A supply the power of 30.09W and 16.49W respectively at this moment. Compared to the required power of existing ankle prosthetic mechanism, as shown in Tab. III, the peak power output of motor in AFP mechanism can be significantly decreased at end of toe-off phase by using TLMS and CCSMP devices.

Spring A can effectively compensate for the biomechanical performance of the mutilated gastrocnemius according to the human-machine simulation in AnyBody software, as shown in Fig.10.

TABLE III
REQUIRED PEAK POWER COMPARISON

Prostheses	Peak power requirements	
	Power	Power density
AFP mechanism	172.86 (W)	2.54 (W/kg)
Knee-ankle prosthesis [27]	307 (W)	2.95 (W/kg)
Ankle-foot prosthesis [28]	274 (W)	3.49 (W/kg)
PANTOE-1st version [24]	251 (W)	3.59 (W/kg)
PANTOE-2nd version [24]	184 (W)	2.63 (W/kg)

The gastrocnemius works to provide power for ankle plantarflexion in gait period. The gastrocnemius medialis provides more muscle force than the gastrocnemius lateralis. However, the damaged gastrocnemius of the transtibial amputees cannot provide enough muscle force during walking and Tab. IV. The gastrocnemius muscles provide 1264N of muscle force for the lower extremity when the human is in prophase of powered plantarflexion, but they can only provide 429.8N of muscle force for the amputated lower limbs.

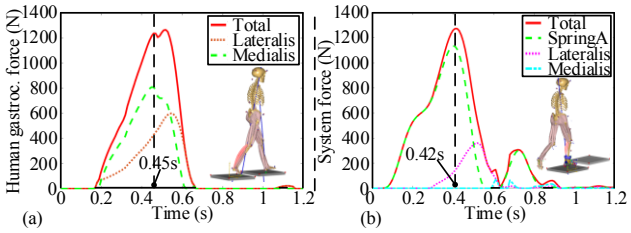

Fig.10. The comparison of gastrocnemius forces of the normal human right shank and the transtibial amputees, as well as the compression spring forces in human-machine system. (a) Gastrocnemius force of human body, (b) Sum of residual gastrocnemius force and pushing force generated by Spring A.

TABLE IV
THE MAXIMUM MUSCLE AND SPRING FORCES DURING GAIT PERIOD

Cases	Human	Human-machine system
gastrocnemius medialis	808 (N)	360 (N)
gastrocnemius lateralis	602 (N)	69.8 (N)
total value	1264 (N)	1271 (N)

In this case, the Spring A of TLMS device compensates the insufficient muscle force for the amputees with AFP mechanism. The compression spring force of 1129N can ensure that the human-like gastrocnemius performance and working conditions during prophase of powered plantarflexion for the human-machine system.

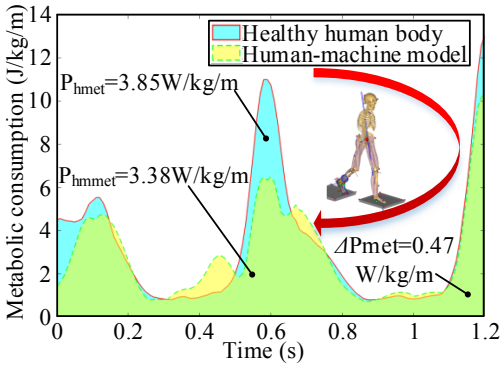

Fig.11. Comparison of the metabolic consumption between human body and human-machine system.

Moreover, the usage of the TLMS device and CCSMP device reduces the metabolic consumption of the transtibial amputees with AFP mechanism, as calculated by human-machine model on AnyBody Modeling System, as shown in Fig.11. Compared with the metabolic consumption of normal human body P_{hmet}= 3.85W/kg/m during walking, the metabolic consumption of AFP mechanism is P_{hmmet}= 3.38W/kg/m, which can save metabolic consumption of ΔP_{met}= 0.47W/kg/m for the transtibial amputees in terms of the human-machine simulation.

V. VERIFICATION PLATFORM SETUP AND EXPERIMENTS

Here we describe the prototype setup to perform kinematic performance evaluation of the designed AFP mechanism.

A. Prototype and Verification Platform

A prototype of the AFP mechanism and its motion function test rig have been built at Beijing Jiaotong University, as shown in Fig.12. The test rig includes hip and knee simulators driven by linear stepper motor (30W, 500N), and they can implement human-like flexion-extension of hip and knee joints based on the referred flexion-extension trajectory of the human hip and knee. This work resolves the difficulty of finding suitable patients with transtibial amputation.

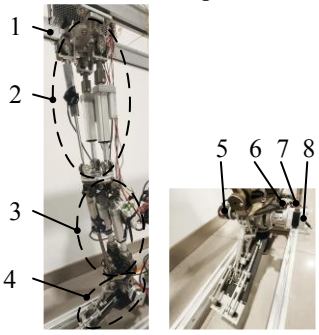

Fig.12. A test rig with a prototype the AFP mechanism. (1) Fixed frame, (2) Hip simulator, (3) Knee simulator, (4) Terminal unit, (5) Driver, (6) Micro-controller, (7) AFP mechanism, (8) Motor, (9) Encoder.

The AFP mechanism weighs 1.78kg and its geometric size is the subjects' average foot. As this work mainly focuses on the

motion functional verification of the AFP mechanism, a DC motor (17W) is used to drive the prosthetic ankle. The motor driver is mainly the microprocessor-controlled ankle has an integrated ankle encoder communicating the ankle position with 1° of resolution via wire at 50Hz. The motor driver is mainly composed of a complete 2-phase 20W DC motor predriver (A4988, Kingroon). Two types of sensors including the inertial measurement units (IMU) and the encoder are used. The encoder is connected to the prosthetic ankle and the position of the prosthetic ankle can be acquired by Arduino UNO board.

B. ATP with position control

In the experiments, the motor was commanded to follow the desired trajectory (θ_{ref}) and a standard PI-controller was used to control the position θ of the prosthetic ankle, as shown the control diagram in Fig.13. Based on the selected motor, the property of motor can be determined which are J=3.23 mg.m^2, B=3.51 μN.m.s, R_a=4 Ω, L_a=2.75 μH, k_1=k=0.03 (N.m)A, and its transfer function in the control system can be determined.

$$\frac{\theta(s)}{U(s)} = \frac{k_1}{(R_a + sL_a)(Js + B) + k_1 ks} \tag{11}$$

where U is motor voltage; R is resistance of motor windings; i_a is current of motor windings; L is motor inductance; e is counter electromotive force; k is back electromotive force constant; k_1 is torque constant; ω is the motor speed; T_e is output torque of motor; T_l is torque under load; B is damping coefficient.

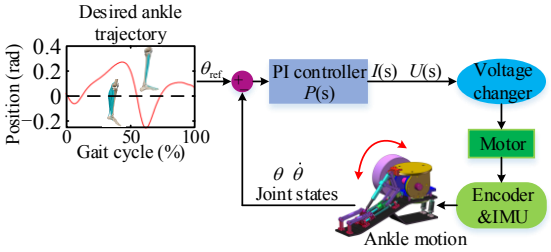

Fig. 13. Schematic diagram of motor control

In this work, the desired motion trajectory comes from measurements of the able-bodied subjects in previous work.

C. Kinematic Verification

The kinematic performance of the AFP mechanism has been tested, as shown in Fig. 14.

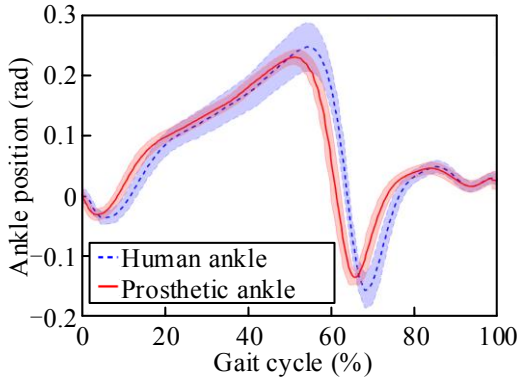

Fig. 14. Kinematic results between human body and prosthetic ankle

It can be seen that the motion trajectory of the AFP mechanism is highly similar to the ankle of able-bodied subjects, and there is a better correlation (r = 0.9204) between them. Regarding differences, motion position of the AFP mechanism presents the root mean square error (RMSD= 0.0398±0.0037 rad) and the relative root mean square error (rRMSE =5.1600±1.4534%) after comparing with the one of the able-bodied subjects [19]. The results show the effectiveness of the AFP mechanism which can be used as the prosthetic ankle for the transtibial amputees.

VI. Discussion and Conclusions

In this work, a novel ATP is presented, which is simple, light weight and compact.

A main contribution of the work is the novel mechanical design of two VSMs, which work with respect to the movements of ankle and toe joints respectively in gait cycle. One of the VSMs named TLMS device, which is a three-loop linkage inspired by the function of muscles agonist-antagonist. The TLMS device functions not only as an energy device to facilitate ankle dorsiflexion-plantarflexion of AFP mechanism in gait cycle, but also a damping device when the amputees' center of gravity tilting forward so that risk of instable walking can be reduced. The other VSM named CCSMP device is a parallel single-loop linkage, which includes a flexible hinge acted as prosthetic toe, so that the AFP mechanism can lift itself by pushing the ground at end of stance phase, and enable an adaptive and flexible contact with the external terrain. The AFP mechanism can be applied to the different amputees with different biomechanical characteristics through adjusting the springs' preload or stiffness of VSMs offline.

Another contribution of the work is the mechanical self-adaptivity of AFP mechanism by using CAB device, which can adjust the posture of lower limbs according to the amputees' center of gravity, so that their walking stability can be improved on the uneven road. Such self-adaptive capacity has not been found in existing prosthesis. The new CAB device can not only improve the stability of level walking, but reduce the impact of prosthetic ankle on uneven terrain.

In conclusion, the presented AFP mechanism enables assisting transtibial amputees to recover their lost bionic ankle with its physiologic characteristics. By comparing theoretical and simulation results, we show that AFP mechanism can perform a human-like ankle dorsiflexion-plantarflexion, and its relationship between ankle position and moment is highly similar with the one of able-bodied subjects. Besides, a prototype is fabricated and its kinematic function is verified, the experimental results show that the correctness of the AFP mechanism development.

This work has potential advantages such as lower peak power of motor with lower metabolic consumption, better kinematic performance and autonomous adaptivity to uneven terrain. In future works, an optimal coupled relationship between human-machine kinematics and kinetics will be explored to optimize the control system, so that the dynamical performances and human-machine biomechanics can be verified to show its design effectiveness. Moreover, mechanical self-adaptive performance of the AFP will be explored experimentally in future work.

REFERENCES

[1] K. Ziegler-Graham, E. J. MacKenzie, P. L. Ephraim, et al., "Estimating the prevalence of limb loss in the United States: 2005- 2050," *Arch. Phys. Med. Rehabil*. vol. 89, no. 3, pp. 422-429, Mar. 2008.

[2] M. Goldfarb, B.E. Lawson, A.H. Shultz, "Realizing the promise of robotic leg prostheses," *Sci. Transl. Med*. vol. 5, no. 210, pp. 210-215, Nov. 2013.

[3] M.R. Pitkin, *Biomechanics of lower limb prosthetics*, Springer-Verlag, Berlin, 2009.

[4] M. Schaarschmidt, S. W. Lipfert, C. Meier-Gratz, et al., "Functional gait asymmetry of unilateral transfemoral amputees," *Hum. Mov. Sci.* vol. 31, no. 4, pp. 907-917, Aug. 2012.

[5] S.K. Au, J. Weber, H. Herr, "Biomechanical design of a powered ankle-foot prosthesis," in *IEEE 10th Int. Conf. Rehabil. Robot.*, Jul. 2007, pp. 298-303.

[6] R.J. Williams, A.H. Hansen, S.A. Gard, "Prosthetic ankle-foot mechanism capable of automatic adaptation to the walking surface," *J. Biomech. Eng.* vol. 131, no. 3, pp. 035002, Apr. 2009.

[7] E. Nickel, J. Sensinger, A. Hansen, "Passive prosthetic ankle-foot mechanism for automatic adaptation to sloped surfaces," *J. Rehabil. Res. Dev.* vol. 51, no. 5, pp. 803-814, Jan. 2014.

[8] M. Grimmer, M. Holgate, R. Holgate, et al., "A powered prosthetic ankle joint for walking and running," *Biomed. Eng. Online* vol. 15, no. 141, pp. 37-52, Dec. 2016.

[9] S.K. Au, P. Dilworth, H. Herr, "An ankle-foot emulation system for the study of human walking biomechanics," in *Proceedings of IEEE International Conference on Robotics and Automation (ICRA)*, Jun. 2006, pp. 2939-2945.

[10] S.K. Au, H. Herr, "Powered ankle-foot prosthesis," *IEEE Rob. Autom. Mag*. vol. 15, no. 3, pp. 52-59, Sep. 2008.

[11] R. Jimenez-Fabian, L. Flynn, J. Geeroms, et al., "Sliding-bar MACCEPA for a powered ankle prosthesis," *J. Mech. Robot.* vol. 7, no. 4, pp. 041011, Nov. 2015.

[12] R. Jimenez-Fabian, J. Geeroms, L. Flynn, et al., "Reduction of the torque requirements of an active ankle prosthesis using a parallel spring," *Rob. Auton. Syst*. vol. 92, pp. 187-196, Jun. 2017.

[13] J. Geeroms, L. Flynn, R. Jimenez-Fabian, et al., "Energetic analysis and optimization of a MACCEPA actuator in an ankle prosthesis energetic evaluation of the CYBERLEGs alpha-prosthesis variable stiffness actuator during a realistic load cycle," *Auton. Robot*. vol. 42, no. 1, pp. 147-158, Jan. 2018.

[14] J. Zhu, Q. Wang, X. Li, et al., "Importance of series elasticity in a powered transtibial prosthesis with ankle and toe joints," in *Proc. IEEE Conf. Robot. Biom. (ROBIO)*, Dec. 2015, pp. 541-546.

[15] Z. Li, S. Bai, O. Madsen, et al., "Design, modeling and testing of a compact variable stiffness mechanism for exoskeletons," *Mech. Mach. Theory* vol. 151, pp. 103905, Sep. 2020.

[16] H. Liu, D. Zhu, J. Xiao, "Conceptual design and parameter optimization of a variable stiffness mechanism for producing constant output forces," *Mech. Mach. Theory* vol. 154, pp. 104033, Dec. 2020.

[17] A. J. Robinson. *Clinical electrophysiology: electrotherapy and electrophysiologic testing*, Lippincott Williams & Wilkins, New York, 2007.

[18] D. A. Winter. *Biomechanics and motor control of human movement*, 3rd ed., Hoboken: John Wiley & Sons, 2005.

[19] M. Damsgaard, J. Rasmussen, S. T. Christensen, et al., "Analysis of musculoskeletal systems in the AnyBody Modeling System," *Simul.Model. Pract. Th.* vol. 14, no. 8, pp. 1100-1111, Nov. 2006.

[20] J.S. Gottschall, R. Kram, "Energy cost and muscular activity required for propulsion during walking," *J. Appl. Physiol.* vol. 94, no. 5, pp. 1766-1772, Jun. 2003.

[21] S. Ounpuu, "The biomechanics of walking and running," *Clin. Sports Med.* vol. 13, no. 4, pp. 843-863, Nov. 1994.

[22] L. Li, D. Zhang, S. Guo, et al., "Design, modeling and analysis of hybrid flexure hinges," *Mech. Mach. Theory* vol. 131, pp. 300-316, Jan. 2019.

[23] L.L. Howell, *Compliant Mechanisms*, John Wiley & Sons, New York, 2001.

[24] J. Zhu, et al. "On the design of a powered transtibial prosthesis with stiffness adaptable ankle and toe joint," *IEEE Trans. Ind. Electron.*, vol. 61, no. 9, pp. 4797-4807, Sep. 2014.

[25] Y. Yu, S. Zhu, "5R pseudo-rigid-body model for inflection beams in compliant mechanisms," *Mech. Mach. Theory*, vol. 116, pp. 501-512, Oct. 2017.

[26] M. Song, S. Guo, A. S. Oliveira, et al., "Design method and verification of a hybrid prosthetic mechanism with energy-damper clutchable device for transfemoral amputees," *Front. Mech. Eng*. vol. 16, no. 4, pp. 747-764, Sep. 2021.

[27] T. Elery, S. Rezazadeh, C. Nesler, et al., "Design and benchtop validation of a powered knee-ankle prosthesis with high-torque, low-impedance actuators," in *IEEE Int. Conf. Robot. Autom. (ICRA)*, May 2018, pp. 2788-2795.

[28] S. K. Au, J. Weber, H. Herr, "Powered ankle-foot prosthesis improves walking metabolic economy," *IEEE Trans.Robot*. vol. 25, no. 1, pp. 51-66, Jan. 2009.